Electronic Supplementary Material (ESI) for Nanoscale.

Electronic Supplementary Information for the paper "Fortune teller fermions in two-dimensional materials" by V. Damljanović, I. Popov and R. Gajić

Classification of linear states in 2D

We first show that in the vicinity of spinless double degenerate point, 2D Dirac bands are the only possible massless bands. Eigenvalues of any two-component, $\boldsymbol{k}$-dependent Hamiltonian $\widehat{H}(\boldsymbol{k})$ are:

$$E_{1,2}(\boldsymbol{k}) = f_0(\boldsymbol{k}) \pm \sqrt{\sum_{j=1}^{3}\left[f_j(\boldsymbol{k})\right]^2}\ , \tag{S1}$$

where

$$(\forall j = \overline{0,3}) f_j(k) = \frac{1}{2} Tr\left[\widehat{H}(\boldsymbol{k})\hat{\sigma}_j\right] \tag{S2}$$

are real functions and $\hat{\sigma}_{1,2,3}$ ($\hat{\sigma}_0$) are the Pauli matrices (is the unit matrix). If $\boldsymbol{k}_0$ is crossing point of two bands and $\boldsymbol{q}$ is a wave vector of small modulus then $f_1(\boldsymbol{k}_0) = f_2(\boldsymbol{k}_0) = f_3(\boldsymbol{k}_0) = 0$ and:

$$E_{1,2}(\boldsymbol{k_0}+\boldsymbol{q}) \approx f_0(\boldsymbol{k_0}+\boldsymbol{q}) \pm \sqrt{u q_1^{2n_1} + v q_2^{2n_2}} \tag{S3}$$

In Eq. (S3), u and v are positive quantities, n_1 and n_2 are natural numbers and q_1 and q_2 are projections of $\boldsymbol{q}$ along certain, mutually orthogonal directions. Since the expression under the square root in Eq. (S3) cannot be negative, the powers on q_1, q_2 must be even. Eq. (S3) is obtained by the Taylor expansion of f_j, (j=1, 2, 3) around the point $\boldsymbol{k}_0$. In order to obtain the effective mass we need second order derivatives with respect to q_1, q_2 at

$\boldsymbol{q}$=0. If x denotes q_1 or q_2, the second derivative of $|x|^n$ (n=2,3,4,..) depends on whether n is even (n=2s, s=1,2,3,..):

$$\frac{d^2}{dx^2}|x|^{2s} = 2s(2s-1)x^{2s-2},$$

or odd (n=2s+1):

$$\frac{d^2}{dx^2}|x|^{2s+1} = 2s(2s-1)|x|^{2s-1} + 4sx^{2s-1}\theta(x) + 2x^{2s}\delta(x).$$

Here $\theta(x)$=1 ($\theta(x)$=-1) for x>0 (x<0) and $\delta(x)$ is Dirac delta-function. For n=2 second derivative at x=0 is a positive constant, which gives rise to finite effective mass. For n>2 second derivative is zero at x=0 and the contribution to the effective mass comes from second derivatives of f_0 in Eq. (S3). Again, the effective mass is finite. The only remaining case n_1=n_2=1 gives zero effective mass and corresponds to 2D Dirac-like dispersion (see Eq. (1) of the main text and this text below).

Next, we classify all possibilities for linear dispersions in the band structure of 2D materials. In order to achieve this aim we define a set of parameters, which values determine possible existence of linear dispersions in 2D crystals. If $G(\boldsymbol{k}_0)$ is the group of the wave vector $\boldsymbol{k}_0$ and R is allowed [32] (relevant [33], small [34]) irreducible representation (irrep) of $G(\boldsymbol{k}_0)$, then the set of parameters consists of

-equivalence of $\boldsymbol{k}_0$ and its inverse $-\boldsymbol{k}_0$,

-dimensionality of representation R,

-reality of representation R.

We consider all possible symmetry groups of crystals which are periodic in 2 spatial directions and finite in the perpendicular direction. These are the so called layer groups (or diperiodic groups). Layer groups have only 1D or 2D allowed irreps [32, 35], while they can be real on one hand or pseudo-real or complex on the other hand. When complex conjugation is a symmetry operation, reality of irreps determines if it causes additional degeneracy. For single crystals the corresponding theory was developed in 1937 [36]. Therefore, each of these parameters can obtain one of two options; hence there are 8 possible combinations, as illustrated in figure S1.

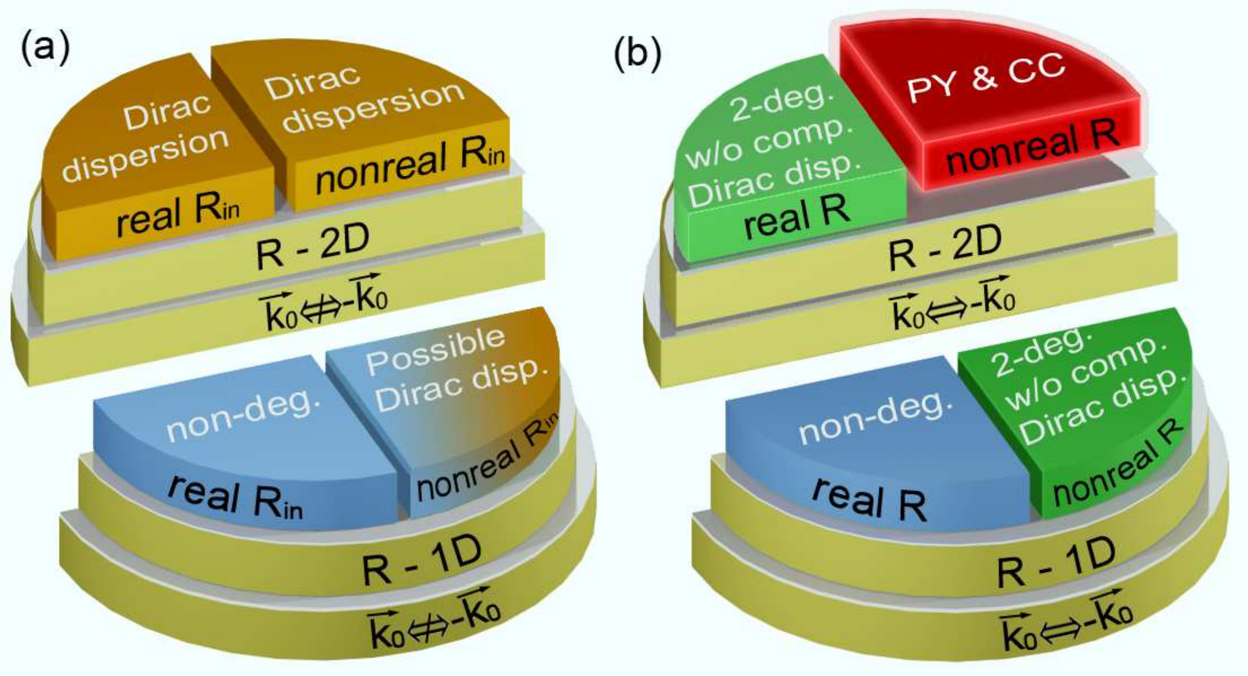

Figure S1. Full classification of linearly dispersive electronic bands in non-magnetic 2D materials based on symmetry conditions. Panel (a) corresponds to the case $\boldsymbol{k}_0 \nLeftrightarrow -\boldsymbol{k}_0$ and panel (b) to the case $\boldsymbol{k}_0 \Leftrightarrow -\boldsymbol{k}_0$. 2-deg. w/o comp. Dirac. disp. means doubly-degeneracy without complete Dirac dispersion, non-deg. means a non-degenerate state.

Firstly, we consider the case $\boldsymbol{k}_0 \nLeftrightarrow -\boldsymbol{k}_0$ (figure S1a). The wave vector $\boldsymbol{k}_0$ must have a locally maximal symmetry, otherwise linear dispersion cannot appear, due to either too many band contacts [S1] or none at all. If R is two-dimensional, and the irrep R_{in} of the whole layer group G, which is obtained by induction from R ($R_{in} = R\uparrow G$) is real, Dirac-like dispersion appears [24] (orange upper left section). If R_{in} is not real, $-\boldsymbol{k}_0$ is not in the star of $\boldsymbol{k}_0$ [32] than the additional degeneracy due to TRS does not appear. This case also leads to Dirac dispersion [24] (orange upper right section). In the last two cases double degeneracy at Dirac point is caused by the crystal symmetry. For R one-dimensional and R_{in} real (left panel blue section), the energy level E_0 at $\boldsymbol{k}_0$ is non-degenerate preventing Dirac dispersion in the vicinity of $\boldsymbol{k}_0$. For R one-dimensional and R_{in} pseudoreal or complex (blue-orange section) there are two possibilities. If $-\boldsymbol{k}_0$ is not in the star of $\boldsymbol{k}_0$, E_0 is non-degenerate while in the opposite case TRS causes E_0 to be double degenerate with a complete Dirac-like dispersion around $\boldsymbol{k}_0$ [25]. Next we consider the case $\boldsymbol{k}_0 \Leftrightarrow -\boldsymbol{k}_0$ (figure S1b). If R is one-dimensional and real, the energy level E_0 at $\boldsymbol{k}_0$ is non-degenerate and linear dispersion cannot appear (right panel blue section). If R is one-dimensional and not real (right panel green section down), TRS causes E_0 to be double degenerate, but complete linear Dirac-like dispersion is not possible since the TRS causes $u_2=0$ (u_2 is a coefficient in the expression for Dirac dispersion [24], see the expression (1) in the main text). The same statement holds for two-dimensional, real R (right panel green section up). The remaining case in which R is two-dimensional and pseudoreal or complex will be treated in more detail in the main text (right panel red section).

Group-theoretical derivations

We show more details in obtaining the dispersion relation (2) of the manuscript. For obtaining irreps *R* of layer single groups we used Bilbao Crystallographic Server [32] for space groups that correspond to the layer single groups of interest. Obtained matrices are given in Tables S1-S3.

Table S1 Matrices of representation U_1 and 2DPV corresponding to *Dg*33. Diperiodic plane is *xz*.

*Dg*33	$(\hat{E}\vert\vec{0})$	$\left(\hat{C}_2^z\middle\vert\frac{1}{2}\vec{a}_3\right)$	$\left(\hat{\sigma}_{xz}\middle\vert\frac{1}{2}\vec{a}_1\right)$	$\left(\hat{\sigma}_{yz}\middle\vert\frac{1}{2}\vec{a}_1+\frac{1}{2}\vec{a}_3\right)$
U_1	$\begin{pmatrix}1 & 0\\ 0 & 1\end{pmatrix}$	$\begin{pmatrix}i & 0\\ 0 & -i\end{pmatrix}$	$\begin{pmatrix}0 & -1\\ 1 & 0\end{pmatrix}$	$\begin{pmatrix}0 & i\\ i & 0\end{pmatrix}$
$\hat{h}'$	$\begin{pmatrix}1 & 0\\ 0 & 1\end{pmatrix}$	$\begin{pmatrix}-1 & 0\\ 0 & 1\end{pmatrix}$	$\begin{pmatrix}1 & 0\\ 0 & 1\end{pmatrix}$	$\begin{pmatrix}-1 & 0\\ 0 & 1\end{pmatrix}$

Table S2 Matrices of representation U_1 and 2DPV corresponding to *Dg*43. Diperiodic plane is *xz*.

*Dg*43	$(\hat{E}\vert\vec{0})$	$\left(\hat{C}_2^z\middle\vert\frac{1}{2}\vec{a}_1\right)$	$\left(\hat{C}_2^y\middle\vert\frac{1}{2}\vec{a}_3\right)$	$\left(\hat{C}_2^x\middle\vert\frac{1}{2}\vec{a}_3-\frac{1}{2}\vec{a}_1\right)$
U_1	$\begin{pmatrix}1 & 0\\ 0 & 1\end{pmatrix}$	$\begin{pmatrix}1 & 0\\ 0 & -1\end{pmatrix}$	$\begin{pmatrix}0 & 1\\ 1 & 0\end{pmatrix}$	$\begin{pmatrix}0 & -1\\ 1 & 0\end{pmatrix}$
$\hat{h}'$	$\begin{pmatrix}1 & 0\\ 0 & 1\end{pmatrix}$	$\begin{pmatrix}-1 & 0\\ 0 & 1\end{pmatrix}$	$\begin{pmatrix}-1 & 0\\ 0 & -1\end{pmatrix}$	$\begin{pmatrix}1 & 0\\ 0 & -1\end{pmatrix}$
*Dg*43	$(\hat{\imath}\vert\vec{0})$	$\left(\hat{\sigma}_{xy}\middle\vert-\frac{1}{2}\vec{a}_1\right)$	$\left(\hat{\sigma}_{xz}\middle\vert-\frac{1}{2}\vec{a}_3\right)$	$\left(\hat{\sigma}_{yz}\middle\vert\frac{1}{2}\vec{a}_1-\frac{1}{2}\vec{a}_3\right)$
U_1	$\begin{pmatrix}0 & -i\\ i & 0\end{pmatrix}$	$\begin{pmatrix}0 & i\\ i & 0\end{pmatrix}$	$\begin{pmatrix}-i & 0\\ 0 & i\end{pmatrix}$	$\begin{pmatrix}-i & 0\\ 0 & -i\end{pmatrix}$
$\hat{h}'$	$\begin{pmatrix}-1 & 0\\ 0 & -1\end{pmatrix}$	$\begin{pmatrix}1 & 0\\ 0 & -1\end{pmatrix}$	$\begin{pmatrix}1 & 0\\ 0 & 1\end{pmatrix}$	$\begin{pmatrix}-1 & 0\\ 0 & 1\end{pmatrix}$

Table S3 Matrices of representation T_1 and 2DPV corresponding to *Dg*45. Diperiodic plane is *yz*.

*Dg*45	$(\hat{E}\vert\vec{0})$	$\left(\hat{C}_2^z\middle\vert\frac{1}{2}\vec{a}_3\right)$	$\left(\hat{C}_2^y\middle\vert\frac{1}{2}\vec{a}_2+\frac{1}{2}\vec{a}_3\right)$	$\left(\hat{C}_2^x\middle\vert\frac{1}{2}\vec{a}_2\right)$
T_1	$\begin{pmatrix}1 & 0\\ 0 & 1\end{pmatrix}$	$\begin{pmatrix}i & 0\\ 0 & -i\end{pmatrix}$	$\begin{pmatrix}-i & 0\\ 0 & -i\end{pmatrix}$	$\begin{pmatrix}1 & 0\\ 0 & -1\end{pmatrix}$
$\hat{h}'$	$\begin{pmatrix}1 & 0\\ 0 & 1\end{pmatrix}$	$\begin{pmatrix}-1 & 0\\ 0 & 1\end{pmatrix}$	$\begin{pmatrix}1 & 0\\ 0 & -1\end{pmatrix}$	$\begin{pmatrix}-1 & 0\\ 0 & -1\end{pmatrix}$
*Dg*45	$(\hat{\imath}\vert\vec{0})$	$\left(\hat{\sigma}_{xy}\middle\vert-\frac{1}{2}\vec{a}_3\right)$	$\left(\hat{\sigma}_{xz}\middle\vert-\frac{1}{2}\vec{a}_2-\frac{1}{2}\vec{a}_3\right)$	$\left(\hat{\sigma}_{yz}\middle\vert-\frac{1}{2}\vec{a}_2\right)$
T_1	$\begin{pmatrix}0 & 1\\ 1 & 0\end{pmatrix}$	$\begin{pmatrix}0 & -i\\ i & 0\end{pmatrix}$	$\begin{pmatrix}0 & -i\\ -i & 0\end{pmatrix}$	$\begin{pmatrix}0 & -1\\ 1 & 0\end{pmatrix}$
$\hat{h}'$	$\begin{pmatrix}-1 & 0\\ 0 & -1\end{pmatrix}$	$\begin{pmatrix}1 & 0\\ 0 & -1\end{pmatrix}$	$\begin{pmatrix}-1 & 0\\ 0 & 1\end{pmatrix}$	$\begin{pmatrix}1 & 0\\ 0 & 1\end{pmatrix}$

We obtain the matrices of representation $D = R \oplus R^*$ from matrices in Tables S1-S3 in the following way. If functions ψ_1 and ψ_2 belong to irreps R from Tables S1-S3, then ψ_1^* and ψ_2^* belong to irrep R^* so functions $\varphi_1 = (\psi_1 + \psi_1^*)/2$, $\varphi_2 = (\psi_1 - \psi_1^*)/(2i)$, $\varphi_3 = (\psi_2 + \psi_2^*)/2$ and $\varphi_4 = (\psi_2 - \psi_2^*)/(2i)$ transform according to the representation D. The final result is given in Tables S4-S6.

Table S4 Matrices of representation *D* corresponding to *Dg*33. Diperiodic plane is *xz*, while $\bar{1} = -1$.

*Dg*33	$(\hat{E}\vert\vec{0})$	$\left(\hat{C}_2^z\middle\vert\frac{1}{2}\vec{a}_3\right)$	$\left(\hat{\sigma}_{xz}\middle\vert\frac{1}{2}\vec{a}_1\right)$	$\left(\hat{\sigma}_{yz}\middle\vert\frac{1}{2}\vec{a}_1+\frac{1}{2}\vec{a}_3\right)$
D	$\begin{pmatrix}1 & 0 & 0 & 0\\ 0 & 1 & 0 & 0\\ 0 & 0 & 1 & 0\\ 0 & 0 & 0 & 1\end{pmatrix}$	$\begin{pmatrix}0 & \bar{1} & 0 & 0\\ 1 & 0 & 0 & 0\\ 0 & 0 & 0 & 1\\ 0 & 0 & \bar{1} & 0\end{pmatrix}$	$\begin{pmatrix}0 & 0 & \bar{1} & 0\\ 0 & 0 & 0 & \bar{1}\\ 1 & 0 & 0 & 0\\ 0 & 1 & 0 & 0\end{pmatrix}$	$\begin{pmatrix}0 & 0 & 0 & \bar{1}\\ 0 & 0 & 1 & 0\\ 0 & \bar{1} & 0 & 0\\ 1 & 0 & 0 & 0\end{pmatrix}$

Table S5 Matrices of representation *D* corresponding to *Dg*43. Diperiodic plane is *xz*, while $\bar{1} = -1$.

*Dg*43	$(\hat{E}\vert\vec{0})$	$\left(\hat{C}_2^z\middle\vert\frac{1}{2}\vec{a}_1\right)$	$\left(\hat{C}_2^y\middle\vert\frac{1}{2}\vec{a}_3\right)$	$\left(\hat{C}_2^x\middle\vert\frac{1}{2}\vec{a}_3-\frac{1}{2}\vec{a}_1\right)$
D	$\begin{pmatrix}1&0&0&0\\0&1&0&0\\0&0&1&0\\0&0&0&1\end{pmatrix}$	$\begin{pmatrix}1&0&0&0\\0&1&0&0\\0&0&\bar{1}&0\\0&0&0&\bar{1}\end{pmatrix}$	$\begin{pmatrix}0&0&1&0\\0&0&0&1\\1&0&0&0\\0&1&0&0\end{pmatrix}$	$\begin{pmatrix}0&0&\bar{1}&0\\0&0&0&\bar{1}\\1&0&0&0\\0&1&0&0\end{pmatrix}$
*Dg*43	$(\hat{\imath}\vert\vec{0})$	$\left(\hat{\sigma}_{xy}\middle\vert-\frac{1}{2}\vec{a}_1\right)$	$\left(\hat{\sigma}_{xz}\middle\vert-\frac{1}{2}\vec{a}_3\right)$	$\left(\hat{\sigma}_{yz}\middle\vert\frac{1}{2}\vec{a}_1-\frac{1}{2}\vec{a}_3\right)$
D	$\begin{pmatrix}0&0&0&\bar{1}\\0&0&1&0\\0&1&0&0\\\bar{1}&0&0&0\end{pmatrix}$	$\begin{pmatrix}0&0&0&1\\0&0&\bar{1}&0\\0&1&0&0\\\bar{1}&0&0&0\end{pmatrix}$	$\begin{pmatrix}0&\bar{1}&0&0\\1&0&0&0\\0&0&0&1\\0&0&\bar{1}&0\end{pmatrix}$	$\begin{pmatrix}0&\bar{1}&0&0\\1&0&0&0\\0&0&0&\bar{1}\\0&0&1&0\end{pmatrix}$

Table S6 Matrices of representation *D* corresponding to *Dg*45. Diperiodic plane is *yz*, while $\bar{1} = -1$.

*Dg*45	$(\hat{E}\vert\vec{0})$	$\left(\hat{C}_2^z\middle\vert\frac{1}{2}\vec{a}_3\right)$	$\left(\hat{C}_2^y\middle\vert\frac{1}{2}\vec{a}_2+\frac{1}{2}\vec{a}_3\right)$	$\left(\hat{C}_2^x\middle\vert\frac{1}{2}\vec{a}_2\right)$
D	$\begin{pmatrix}1&0&0&0\\0&1&0&0\\0&0&1&0\\0&0&0&1\end{pmatrix}$	$\begin{pmatrix}0&1&0&0\\\bar{1}&0&0&0\\0&0&0&\bar{1}\\0&0&1&0\end{pmatrix}$	$\begin{pmatrix}0&\bar{1}&0&0\\1&0&0&0\\0&0&0&\bar{1}\\0&0&1&0\end{pmatrix}$	$\begin{pmatrix}1&0&0&0\\0&1&0&0\\0&0&\bar{1}&0\\0&0&0&\bar{1}\end{pmatrix}$
*Dg*45	$(\hat{\imath}\vert\vec{0})$	$\left(\hat{\sigma}_{xy}\middle\vert-\frac{1}{2}\vec{a}_3\right)$	$\left(\hat{\sigma}_{xz}\middle\vert-\frac{1}{2}\vec{a}_2-\frac{1}{2}\vec{a}_3\right)$	$\left(\hat{\sigma}_{yz}\middle\vert-\frac{1}{2}\vec{a}_2\right)$
D	$\begin{pmatrix}0&0&1&0\\0&0&0&1\\1&0&0&0\\0&1&0&0\end{pmatrix}$	$\begin{pmatrix}0&0&0&\bar{1}\\0&0&1&0\\0&1&0&0\\\bar{1}&0&0&0\end{pmatrix}$	$\begin{pmatrix}0&0&0&\bar{1}\\0&0&1&0\\0&\bar{1}&0&0\\1&0&0&0\end{pmatrix}$	$\begin{pmatrix}0&0&\bar{1}&0\\0&0&0&\bar{1}\\1&0&0&0\\0&1&0&0\end{pmatrix}$

Group projector to the totally symmetric irreducible representation is given by:

$$\hat{P} = \frac{1}{|G(\boldsymbol{k}_0)|}\sum \hat{D}\otimes\hat{D} \otimes \hat{h}'$$

where the sum is over little group elements $G(\boldsymbol{k}_0)$. In our three cases this included the whole layer single group. Obtained projection operator is 32-dimensional. By applying $\hat{P}$ to general 32-component vector consistent with TRS-constrained matrix $\widehat{W}$:

$$\widehat{W} = i\begin{pmatrix} 0 & \langle \boldsymbol{v}_1| & \langle \boldsymbol{v}_2| & \langle \boldsymbol{v}_3| \\ -\langle \boldsymbol{v}_1| & 0 & \langle \boldsymbol{v}_4| & \langle \boldsymbol{v}_5| \\ -\langle \boldsymbol{v}_2| & -\langle \boldsymbol{v}_4| & 0 & \langle \boldsymbol{v}_6| \\ -\langle \boldsymbol{v}_3| & -\langle \boldsymbol{v}_5| & -\langle \boldsymbol{v}_6| & 0 \end{pmatrix},$$

we get symmetry constrained vectors $\boldsymbol{v}_j$. Final result is given in the Table S7.

Table S7 Form of vectors $\boldsymbol{v}_j$ $(j = 1,2,\ldots,6)$ required by symmetry, for the layer single groups *Dg*33, *Dg*43 and *Dg*45. Components of vectors are along ***a***- and ***c***-axes for groups *Dg*33 and *Dg*43, and ***b***- and ***c***-axes for group Dg45 respectively. The ***a***-, ***b***- and ***c***-axes are orthorhombic axes for corresponding space groups 29, 54 and 57 respectively.

	*Dg*33	*Dg*43	*Dg*45
$\boldsymbol{v}_1$	$\begin{pmatrix} 0 \\ v_{1c} \end{pmatrix}$	$\begin{pmatrix} 0 \\ v'_{1c} \end{pmatrix}$	$\begin{pmatrix} 0 \\ 0 \end{pmatrix}$
$\boldsymbol{v}_2$	$\begin{pmatrix} v_{2a} \\ v_{2c} \end{pmatrix}$	$\begin{pmatrix} v'_{2a} \\ 0 \end{pmatrix}$	$\begin{pmatrix} v''_{2b} \\ v''_{2c} \end{pmatrix}$
$\boldsymbol{v}_3$	$\begin{pmatrix} 0 \\ v_{3c} \end{pmatrix}$	$\begin{pmatrix} v'_{3a} \\ 0 \end{pmatrix}$	$\begin{pmatrix} 0 \\ v''_{3c} \end{pmatrix}$
$\boldsymbol{v}_4$	$\begin{pmatrix} 0 \\ v_{3c} \end{pmatrix}$	$\begin{pmatrix} v'_{3a} \\ 0 \end{pmatrix}$	$\begin{pmatrix} 0 \\ v''_{3c} \end{pmatrix}$
$\boldsymbol{v}_5$	$\begin{pmatrix} v_{2a} \\ -v_{2c} \end{pmatrix}$	$\begin{pmatrix} -v'_{2a} \\ 0 \end{pmatrix}$	$\begin{pmatrix} v''_{2b} \\ -v''_{2c} \end{pmatrix}$
$\boldsymbol{v}_6$	$\begin{pmatrix} 0 \\ v_{1c} \end{pmatrix}$	$\begin{pmatrix} 0 \\ -v'_{1c} \end{pmatrix}$	$\begin{pmatrix} 0 \\ 0 \end{pmatrix}$

If we insert values for $\boldsymbol{v}_j$ into the Eq. (9) of the main text, we get the dispersion (2). Note that the form of Hamiltonian $\widehat{H}'$ required by the Table S7 is valid only in the basis that belongs to the representation *D* given in Tables S4-S6. On the other hand, eigenvalues of $\widehat{H}'$ are invariant, and are therefore the same in every basis.

The effective mass calculation

Next we show that the dispersion (2) leads to zero effective mass. We take the dispersion for $E_1(\boldsymbol{q})$, obtained from Eq. (2) of the main manuscript by taking plus signs, as an example. The proof for other bands, including Dirac-like (1) is analogous. Let us define the matrix:

$$\hat{S}(q_1, q_2) = \begin{pmatrix} \frac{\partial^2}{(\partial q_1)^2} E_1(q_1, 0) & \left[\frac{\partial^2}{\partial q_1 \partial q_2} E_1(q_1, q_2)\right]_{q_2=0} \\ \left[\frac{\partial^2}{\partial q_2 \partial q_1} E_1(q_1, q_2)\right]_{q_1=0} & \frac{\partial^2}{(\partial q_2)^2} E_1(0, q_2) \end{pmatrix}.$$

The matrix element $\left[\frac{\partial^2}{\partial q_1 \partial q_2} E_1(q_1, q_2)\right]_{q_2=0}$ means that firstly we take the derivative with respect to q_2, than take $q_2=0$, and then take derivative with respect to q_1 (and analogously for the other off-diagonal element). The matrix $\hat{S}$ in terms of Dirac delta function reads:

$$\hat{S}(q_1, q_2) = \begin{pmatrix} 2u_1\delta(q_1) & 0 \\ 0 & 2u_2\delta(q_2) \end{pmatrix}.$$

Function $E_1(q_1, q_2)$ has minimum for $q_1 = q_2 = 0$, so the effective mass tensor is:

$$\widehat{\mathrm{m}}_{\mathrm{eff}} = \hbar^2 \left[\hat{S}(q_1, q_2)\right]^{-1} |_{q_1=q_2=0}.$$

Using the interpretation of delta-function as being infinite at zero, we get $\widehat{\mathrm{m}}_{\mathrm{eff}} = \hat{0}$.

The density of states calculation

Here we show how one obtains the density of states (DOS) for FT dispersion, starting from the general definition of DOS. First we define:

$$\varepsilon_+ = \big|u_1|q_1| + u_2|q_2|\big|,$$

$$\varepsilon_- = \big|u_1|q_1| - u_2|q_2|\big|.$$

The definition for DOS reads:

$$\rho_\pm(\varepsilon) = \frac{1}{4\pi^2}\int_{-\frac{\pi}{a}}^{\frac{\pi}{a}} dq_1 \int_{-\frac{\pi}{b}}^{\frac{\pi}{b}} dq_2\, \delta(\varepsilon - \varepsilon_\pm(q_1, q_2)) =$$

$$= \frac{1}{\pi^2}\int_0^{\frac{\pi}{a}} dq_1 \int_0^{\frac{\pi}{b}} dq_2\, \delta(\varepsilon - \varepsilon_\pm(q_1, q_2)),$$

where we have reduced integration to the first quadrant. We introduce the substitution:

$$q_1 = \frac{1}{2u_1}x + \frac{1}{2u_1}y,$$

$$q_2 = \frac{1}{2u_2}x - \frac{1}{2u_2}y,$$

with the corresponding modulus of Jacobian determinant $|J| = \frac{1}{2u_1u_2}$. The range of integration in new variables becomes:

$$0 \leq x \leq u_1\frac{\pi}{a} + u_2\frac{\pi}{b},$$

$$-\frac{\pi u_2}{b} \leq y \leq \frac{\pi u_1}{a}.$$

It follows:

$$\rho_+(\varepsilon) = \frac{1}{2u_1u_2\pi^2}\int_0^{u_1\frac{\pi}{a}+u_2\frac{\pi}{b}} dx \int_{-\frac{\pi u_2}{b}}^{\frac{\pi u_1}{a}} dy\, \delta(\varepsilon - x) =$$

$$= \begin{cases} \frac{1}{2u_1u_2\pi}\left(\frac{u_1}{a}+\frac{u_2}{b}\right); 0 < \varepsilon < \frac{\pi u_1}{a}+\frac{u_2\pi}{b} \\ \frac{1}{4u_1u_2\pi}\left(\frac{u_1}{a}+\frac{u_2}{b}\right); \varepsilon = 0 \\ 0; \varepsilon < 0 \end{cases}$$

which, after taking in account the particle-hole symmetry for bands $\pm\varepsilon_+$, gives:

$$\rho_1(\varepsilon) = \frac{1}{2u_1u_2\pi}\left(\frac{u_1}{a}+\frac{u_2}{b}\right),$$

for sufficiently small $|\varepsilon|$. Similarly, we get for ε_-:

$$\rho_-(\varepsilon) = \frac{1}{2u_1u_2\pi^2}\int_0^{u_1\frac{\pi}{a}+u_2\frac{\pi}{b}} dx \int_{-\frac{\pi u_2}{b}}^{\frac{\pi u_1}{a}} dy\, \delta(\varepsilon - |y|) =$$

$$= \begin{cases} \frac{1}{u_1u_2\pi}\left(\frac{u_1}{a}+\frac{u_2}{b}\right); 0 < \varepsilon < min\left\{\frac{\pi u_1}{a}, \frac{u_2\pi}{b}\right\} \\ \frac{1}{2u_1u_2\pi}\left(\frac{u_1}{a}+\frac{u_2}{b}\right); \varepsilon = 0 \\ 0; \varepsilon < 0 \end{cases}.$$

Particle-hole symmetry for bands $\pm\varepsilon_-$ implies, for sufficiently small $|\varepsilon|$:

$$\rho_2(\varepsilon) = \frac{1}{u_1u_2\pi}\left(\frac{u_1}{a}+\frac{u_2}{b}\right).$$

After the inclusion of spin degeneracy, and using $u_1 = \hbar v_a$, $u_2 = \hbar v_b$, the total DOS for small $|\varepsilon|$ reads, in terms of Fermi velocities:

$$\rho(\varepsilon) \approx \frac{3}{\pi\hbar}\left(\frac{1}{av_b}+\frac{1}{bv_a}\right).$$

Algorithm used in ab initio search

1. **One chemical element is chosen** from the main groups of the periodic table (IIIA, IVA and VA). Particularly we considered B, C, Si or P.
2. **Setup of initial parameters.** Initial fractional coordinates of a single atom, lattice vectors and one of diperiodic groups, Dg33, Dg43 or Dg45, are chosen. The initial lattice vectors and coordinates are chosen such that bond lengths in the system are as close as possible to typical bond lengths between atoms of a given element. This is done manually. Set up the initial value of variable *current minimal energy* to a large value, i.e. DBL_MAX (predefined value in the C++ language standard). Set up the initial *scaling factors* for lattice vectors. Value of 0.8 was a usual choice.
3. Scale lattice vectors by the current *scaling factors*.
4. Atomic positions of remaining atoms in a unit cell are generated based on Wyckoff equivalent positions for the chosen group.
5. **Screening of possibly stable geometries.** The generated crystal structure (from combination of fractional coordinates and scaled lattice vectors) is checked if it is *likely* stable by analyzing eventual clustering of its atomic positions to disjoined set of clusters. The structure is assumed as unstable and disregarded for further calculations if it has more than 2 disjoined clusters. Two clusters are considered disjoined, if distance between two atoms closest to each other, but belonging to different clusters, is larger or smaller by more than n Å than the sum of their covalent radii. n = 0.3 Å was usually used for most of elements. Larger values of

n up to 0.5 Å are used for carbon, for which it is known to make a larger range of possible bond lengths. This step is done in order to speed up the search of stable structures.

6. **Symmetry-constrained geometry optimization.** If the given structure is not disregarded at the step 5 as an unsuitable initial geometry, a geometry optimization is conducted with constrained diperiodic group, i.e. its corresponding space group. Otherwise, go to the step 9. Density functional theory (DFT)-based software Siesta [S2] is used for calculations of energies and atomic forces during the group-constrained geometry optimization.
7. **Can the symmetry be preserved?** Full unconstrained structural optimization is conducted using the Siesta code. Initial geometry for the optimization is the geometry obtained at the step 6. The optimized geometry is checked for eventual breaking of the symmetry (the diperiodic group, i.e. its corresponding space group) after the full structural optimization. Also check the structural stability of the crystal using the same method described at the step 5.
8. If the symmetry is preserved and the structural stability is confirmed at the step 7, compare total energy with the *current minimal energy*. If it is a smaller one then promote it to the *current minimal energy*, and save atomic coordinates of this structure.
9. Increase scaling factors by 0.02. If they are smaller than 1.2 return to the step 3. Otherwise continue to the step 10.
10. Calculate electronic band structure for the most stable system (*current minimal*) using the Siesta code and analyze the band structure.

All *ab initio* calculations were done using DFT as implemented in the Siesta code [S2]. Space groups from Table 1 were used, which correspond to diperiodic groups, when unit cells were constructed. Lattice vector perpendicular to diperiodic plane was always 15 Å. We utilized the Perdew-Burke-Ernzerhof form of the exchange-correlation functional [S3]. The behavior of valence electrons was described by norm-conserving Troullier-Martins pseudopotential [S4]. We used a double-zeta polarized basis. The mesh cutoff energy of 250 Ry was used, which was sufficient to achieve a total energy convergence of better than 0.1 meV per unit cell during the self-consistency iterations of all calculations. Structures were considered as optimized when maximal force on atoms dropped below 0.04 eV/Å. In the search algorithm a 8 x 8 k-point Monkhorst-Pack mesh in plane of BZ corresponding to the plane of 2D materials was employed and only gamma point was used in the perpendicular direction. A denser k-point mesh of 12 x 12 was used for further optimization and calculation of band structure and density of states of the most stable structures obtained by the search algorithm.

Bands in Fig. 2(b) were obtained on 300 x 300 k-point grid around the corner of BZ (point R).

Molecular dynamics simulation, which confirmed the structural stability of P (Dg45) system, was conducted for 5 ps in 5000 steps of 1fs. Temperature was fixed at 100 K using the Nosé-Hoover thermostat. A super-cell comprising 3 x 3 x 1 repetition of a unit cell containing 36 P atoms was employed in the simulation.

ADDITIONAL REFERENCES

[S1] Wang, J.; Huang, H.; Duan, W.; Liu, Z. Identifying Dirac cones in carbon allotropes with square symmetry *J. Chem. Phys.* 2013, **139,** 184701

[S2] Soler. J. M.; Artacho, E.; Gale, J. D.; Garcia, A.; Junquera, J. P.; Ordejon, P.; Sanchez Portal. The SIESTA method for ab initio order-N materials simulation. *J. Phys. Cond. Mat.* 2002, **14**, 2745-2779.

[S3] Perdew, J. P.; Burke, K.; Ernzerhof, M. Generalized gradient approximation made simple. *Phys. Rev. Lett.* 1996, **77**, 3865-3868.

[S4] Troullier, N.; Martins, J. L. Efficient pseudopotentials for plane-wave calculations. *Phys. Rev. B* 1991, **43**, 1993-2006.